Qualitative and quantitative analysis of atmospheric methanol using a continuous-wave terahertz spectrometer

Han Zhang (张 寒)[1,2], Zhaohui Zhang (张朝晖)[2,3,*], Xiaoyan Zhao (赵小燕)[3], Xiaotong Zhang (张晓彤)[1], Tianyao Zhang (张天尧)[3], Can Cao (曹 灿)[3], and Yang Yu (于 洋)[3]

[1]*School of Computer and Communication Engineering, University of Science and Technology Beijing, Beijing 100083, China*

[2]*Beijing Engineering Research Center of Industrial Spectrum Imaging, Beijing 100083, China*

[3]*School of Automation and Electrical Engineering, University of Science and Technology Beijing, Beijing 100083, China*

**Corresponding author: zhangzhaohui@ustb.edu.cn*

Received July 9, 2018; accepted August 30, 2018; posted online September 20, 2018

We present a specific-window method to subtract the interference of water vapor on terahertz frequency-domain spectroscopy (THz-FDS) at ambient temperature and pressure. A continuous-wave spectrometer based on photomixing was utilized to obtain THz-FDS of methanol vapor in the range of 50–1200 GHz. The distinctly spaced absorption features in the neighborhood of atmospheric windows of transparency were selected to perform linear fitting versus the calculated absorption cross section and obtain the concentration of methanol. Furthermore, the gradually decreased methanol vapor was quantified to demonstrate the reliability of the method.

OCIS codes: 300.6495, 300.6390, 300.1030, 010.1120.
doi: 10.3788/COL201816.103001.

The qualitative and quantitative analysis of pollution gas in atmosphere is vital to environmental monitoring. Since the terahertz (THz) wave is sensitive to many gas species, more and more research efforts have been devoted to the development of spectroscopic THz gas sensors[1]. However, the monitoring and analysis of gas in the atmosphere is far from practical application, since much interference is unavoidable, for instance, the atmospheric water vapor strongly attenuates the THz radiation.

It is worth mentioning that some studies concerning the application in real atmosphere have been reported. Hsieh *et al.*[2] utilize asynchronous-optical-sampling THz time-domain spectroscopy (THz-TDS) with a resolution of 1 GHz to achieve a detect limit of 200 ppm (1 ppm = 10^{-6}) for acetonitrile (CH_3CN) gas in the presence of smoke under atmospheric pressure, which undoubtedly proves that THz spectroscopy is a promising method for environmental monitoring. The non-mechanical time-delay scanning in this method provides more advantages on spectral resolution, accuracy, and measurement time than the conventional THz-TDS. The cost is the simultaneous water vapor that has to also be quantified.

Another major THz spectroscopy is the THz frequency-domain spectroscopy (THz-FDS), realized by frequency scanning narrow-band continuous-wave THz radiation. The latest study released by Tekawade *et al.*[3] explores the potential of THz wave electronics for measuring methanol in ambient air at 500 Torr total pressure within the 220–330 GHz region using a radio-frequency multiplier source. Although the frequency band is narrow, such that the interference from water vapor is not included, this might lose some spectral features and is limited by less gas species that can be detected.

THz-FDS obtained by the photomixing technique is another promising approach to achieving broader continuous tuning range of sub-THz to THz order while maintaining moderate spectral resolution. Recently, optical frequency combs (OFCs) have combined with the photomixing technique to achieve higher frequency accuracy, stability, and resolution at some expense of bandwidth. With this technique the CH_3CN gas is investigated but under very low pressure[4].

Since there are limited researches on gas in real atmosphere, this work aims to explore the feasibility of high-sensitivity measurement of target gas under normal pressure and temperature. In this study, a fiber-based photomixing THz spectrometer with a broad bandwidth was utilized to detect methanol vapor with various concentrations in the atmosphere. The important point is that we do not purge the water vapor before experiments but utilize a specific-window method, which chooses several atmospheric windows of transparency to perform the quantitative analysis.

Continuously tunable measurements were performed on a TOPTICA TeraScan 1550 platform. As shown in Fig. 1, the interference of the beams from two distributed feedback (DFB) lasers generated a laser beat, one splitting beam of which irradiated on the InGaAs photomixer to generate a THz wave. A coherent detection scheme was applied; the THz wave was focused into the InGaAs detector, and meanwhile, another splitting beam of the laser beat irradiated on the detector. The induced photocurrent

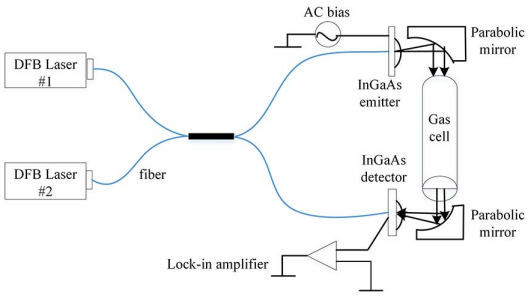

Fig. 1. Schematic diagram of THz-FDS system for gas detection.

proportional to the amplitude of the THz electric field was then amplified by a lock-in amplifier. The AC biased voltage with a modulation frequency of ∼39.67 kHz was supplied to the THz emitter, as required for lock-in detection. A full scan from 50 to 1200 GHz was finished in 2 min. Rather than using a mechanical delay line, an interference pattern[5] was obtained by scanning the THz frequency in a small step. The envelope of the interference pattern was extracted to yield the THz spectrum with an uncertainty of frequency of ∼10 MHz, and the effective resolution was about 1.5 GHz, which was determined by the difference between the optical path traveled by the laser beat to the detector and the optical path of the laser beat to the THz source together with the THz path from the source to the detector. A homemade cylindrical organic glass chamber was used as a gas cell. Both sides of the gas cell were sealed with 1 mm thick white polytetrafluoroethylene (PTFE) sheets, which were located perpendicular to the radiation transmission direction. A pair of gold-coated 90° off-axis parabolic mirrors (OAPs) with 1 in. (2.54 cm) in diameter was used to collimate and focus the THz wave. The gas cell is 20 cm long and has an inner diameter of 5.7 cm, which can enable the collimated THz beam to completely go through the cell. The dynamic range of the THz signal without and with the gas cell placed was calculated at frequency ν by $\mathrm{DR} = 20 \times \lg[I_{\mathrm{signal}}(\nu)/I_{\mathrm{noise}}]$, as shown in Fig. 2, in which I_{noise}, the root mean square (RMS) value of the 100 photocurrent data points measured by setting the amplitude of bias voltage to zero, was 192 pA. The dips in the graph are water lines. The experimental relative humidity was about 30%, and the temperature was 23.5 ± 0.2°C. The dynamic range of the gas cell declines a bit compared to the air spectrum, which demonstrates the good transparency of PTFE windows.

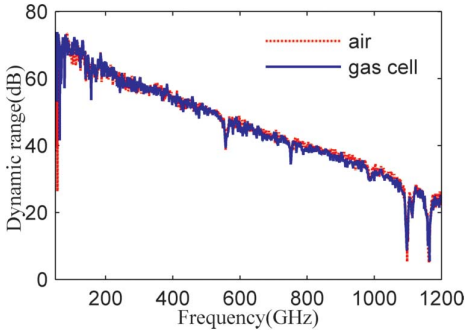

Fig. 2. Dynamic range of scanning THz signal of air (dashed line) and vacant gas cell (solid line).

Methanol is one of the most abundant oxygenated volatile organic compounds in the atmosphere[6]. We selected methanol as a sample gas to demonstrate the capability of the THz-FDS system to simultaneously probe multiple absorption lines. First, a series of scans of the vacant gas cell was collected as a reference. The liquid methanol (Amethyst Chemicals) has a purity of 99.9%. About 0.25 mL of methanol was injected into the gas cell through the outlet on the chamber wall, and the completely vaporized methanol was analyzed. For both reference and sample, the THz spectrum was an average of three scanning signals, as shown in Fig. 3.

The qualitative and quantitative analysis was carried out by comparing experimental and theoretical absorbance. The experimental absorbance $\alpha(\nu)$ was obtained by the Lambert–Beer law as

$$T(\nu) = \exp[-\alpha(\nu)], \tag{1}$$

where the transmittance[7] can be calculated by $T(\nu) = [I_{\mathrm{sam}}(\nu)/I_{\mathrm{ref}}(\nu)]^2$, in which I_{sam} and I_{ref} are the amplitudes of sample and reference, respectively, in Fig. 3. The theoretical absorbance can be defined as[6]

$$\alpha(\nu) = N_s L \sigma(\nu). \tag{2}$$

In Eq. (2), N_s is the number density of the absorbing species (molecule/cm^3); L is the length of the gas cell (cm); $\sigma(\nu) = \sum_k S_k F(\nu, \nu_k)$ is the absorption cross section (cm^2/molecule) with the line intensity S_k at the transition frequency ν_k broadened by the line profile $F(\nu, \nu_k)$ and then added up in the desired frequency range. Clearly there is a linear relation between the absorbance and the number density in Eq. (2) once the absorption cross section is determined.

Stimulated by recent THz developments, the spectral line parameters of methanol have been reported in THz frequency[6,8]. The line intensity and transition center frequency in the Cologne Database for Molecular Spectroscopy (CDMS)[9] were used to calculate the absorption cross section. Firstly, the unit of line intensity, 1 nm^2 · MHz at 300 K, was transformed into 1 cm^{-1}/(molecule · cm^{-2}) at 296 K using Eq. (11) in Ref. [10]. In the frequency range of

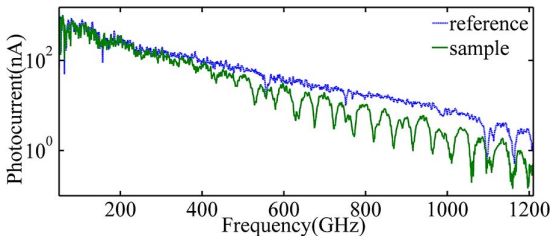

Fig. 3. Averaged amplitude of THz electric field signal of methanol sample (bottom) and reference (top).

100–1200 GHz, half-width at half-maximum (HWHM) of methanol broadened by the Doppler effect was less than 1.3 MHz. The pressure broadening width is a few gigahertz (GHz)[4,6]. Therefore, the pressure broadening is dominant, and the line broadening can be described by the Lorentz profile:

$$F(\nu,\nu_k)=\frac{1}{\pi}\left[\frac{\Delta\nu_k}{(\nu-\nu_k)^2+\Delta\nu_k^2}\right], \tag{3}$$

in which the half-width $\Delta\nu_k$ can be established by $\Delta\nu_k=\gamma_{k-\mathrm{air}}P_{\mathrm{air}}$. The air-broadening coefficient $\gamma_{k-\mathrm{air}}$ fixed at 0.1 $\mathrm{cm}^{-1}\cdot\mathrm{atm}^{-1}$ in the high-resolution transmission molecular absorption (HITRAN) database compiled by Rothman *et al.*[11] was adopted. The air pressure P_{air} was nearly 1 atm. Therefore, for all of the transition center frequencies, we have utilized a fixed half-width value of 0.1 cm^{-1}. It should be noted that owing to the small amount of methanol vapor, the self-broadening width has been neglected. The air-induced line shift has not been taken into account due to lack of data. The temperature-dependence exponent was not considered either.

Figure 4 shows the computed absorption cross section compared with the experimental absorbance. The frequency range was selected below 1090 GHz due to the strong water lines at 1097, 1113, and 1164 GHz, as can be observed in Fig. 3. From the comparison between experimental and theoretical absorption, we assigned the absorption peaks in the range of 384.4–1061 GHz to the energy level from $J=7$ to $J=21$, where J is the total angular momentum quantum. Also, we can notice that the sample features distribute at approximate equal distance. That is because methanol is nearly a prolate symmetric top molecule with rotational constants: $A=127523.4$ MHz, $B=24692.5$ MHz, and $C=23760.3$ MHz[9], and the frequency spacing approaches the effective rotational constant[12]: $B+C=48452.8$ MHz.

For the quantitative analysis, according to Eq. (2), a linear regression can be performed on the absorbance peak versus the corresponding absorption cross section multiplied by path length L to obtain the number density of methanol. However, the water lines reproduced in the original sample signal would affect the experimental absorbance. As can be seen in Fig. 3, the absorption at 557.6 GHz in the sample signal should arise from water, since no strong methanol absorption lines exist at this point, as revealed from the absorption cross section in Fig. 4. The existence of water lines in the sample signal cannot completely counteract that in the reference signal because the sample signal had less relative amount of water vapor owing to the addition of methanol. Therefore, negative absorption values will arise at the water line positions during the experimental absorbance calculation, which is evident from the point at 557.6 GHz denoted in Fig. 4.

To subtract the response due to water vapor, several frequency sub-bands were selected in the neighborhood of transparent windows to perform the linear regression. Nine absorption peaks of methanol at 384.4 ($J=7$), 434.2 ($J=8$), 629 ($J=12$), 636.4, 674.6 ($J=13$), 819.6 ($J=16$), 869.2 ($J=17$), 890.2, and 915.8 ($J=18$) GHz around the transparent windows centered at 0.41, 0.68, 0.85, and 0.94 THz[13] were selected. All of the distances from these peaks to the closest window center were within approximately 50 GHz. Other peaks at 481.4, 528, 579.6, 722.4, 758.4, 770.6, 964, 1011, and 1059 GHz on the wings of water lines (557.6, 751, 989.4, and 1097 GHz) had been removed. These removed

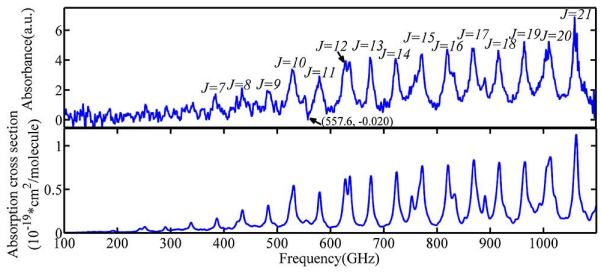

Fig. 4. Calculated absorption cross section (bottom) from 100 to 1090 GHz compared with the experimental absorbance (top).

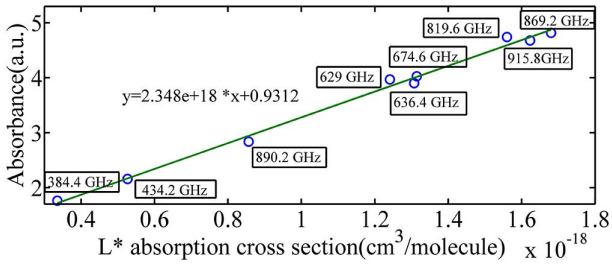

Fig. 5. The linear regression on the absorption peaks of methanol.

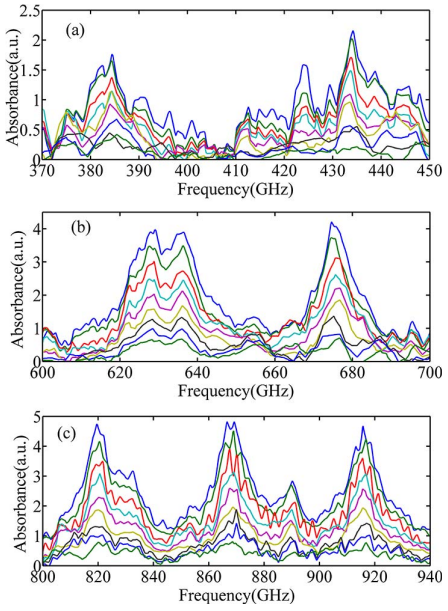

Fig. 6. Three frequency sub-bands of absorbance spectra of nine samples with gradually reduced methanol vapor.

Table 1. Linear Regression Results and Correctness of Fitting

Sample No.	Concentration (molecule/cm^3)	Adjusted R^2 Coefficient	RMSE
1	2.348×10^{18}	0.9926	0.09824
2	2.061×10^{18}	0.9939	0.07799
3	1.793×10^{18}	0.9678	0.15790
4	1.488×10^{18}	0.9891	0.07557
5	1.245×10^{18}	0.9859	0.07203
6	7.186×10^{17}	0.9165	0.10430
7	8.854×10^{17}	0.8943	0.14610
8	4.283×10^{17}	0.6642	0.14280
9	3.922×10^{17}	0.8504	0.07868

points even include absorption peaks on the far wings of water lines, since we suppose that the continuum attenuation due to broadening of strong water lines[13] should be removed as well. All of these points except that at 481.4 GHz have a distance of less than 38 GHz to the center of the closest water line. The distance from the absorption at 481.4 GHz to the window at 0.41 THz and the water line at 557.6 GHz was nearly equal, yet it was still removed to make the data more reliable. Three peaks in the range of 200–350 GHz in our study were too weak to consider. In Fig. 5, the linear regression curve for the selected absorption peaks is shown. The slope represents the number density, and the intercept indicates other contributions to absorption.

To further investigate the capacity of the THz-FDS system, we varied the sample concentration by outgassing for 10 or 15 min, while attaching the outside wall with a rectangular heat plate of 8 cm × 3 cm at 40°C to speed up the process. After the system had come to equilibrium, a sample scan was completed. Repeating the above process, a total of nine samples (samples 1 to 9) with gradually reduced methanol concentrations were obtained, and their absorbance spectra are shown in Fig. 6 within three different frequency sub-bands, where significant decline of absorption can be observed.

Table 1 shows the fitting results for all of the samples exhibiting good linear relations in general by comparing the adjusted R^2 coefficients and RMS errors (RMSEs). However, there exists an exception for the concentration of sample 7, which should be lower. That is probably due to the weak absorption of the sample. As can be seen in Fig. 6, the absorption spectra appear non-uniform, especially for the lower frequency band of 370–450 GHz, which might be due to the photocurrent noise, and this will have more influence on the weak absorption sample with lower concentration.

Although we can only confirm that the lower detection limit of methanol is less than the concentration of sample 9, which is large in this study, the present measurements are the result of a single-pass gas cell, and the detection limit can be greatly decreased by increasing the optical path length. In addition, to evaluate the sensing threshold of the whole system including the gas chamber, we scanned ten sets of vacant chamber signals and calculated their relative standard deviation (RSD) for each frequency over the range of 300–1000 GHz, as shown in Fig. 7. The average of the RSD in this range is 2.2%, corresponding to a minimum absorption coefficient of 0.002 cm^{-1}.

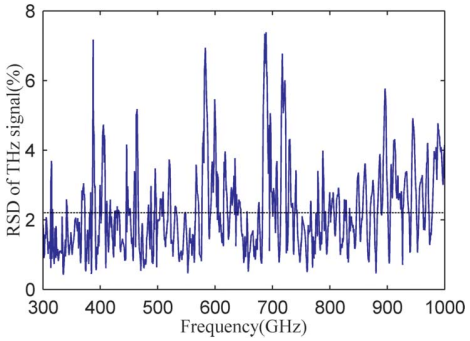

Fig. 7. Relative standard deviation (RSD) of THz signal for vacant chamber.

In conclusion, four specific windows of transparency below 1 THz were utilized to remove the interference of water lines under normal pressure and temperature. Based on the method, qualitative and quantitative analyses of methanol samples with various concentrations in atmosphere were performed, which exhibit consistent absorption features and good regression results. The stability and frequency selectivity of this method based on the fast scanning THz-FDS have been demonstrated. However, with the decreased methanol, the goodness of fitting declined due to the weak absorption of samples. Increasing the length of the gas chamber and more precise absorption cross section calculations would improve the sensitivity and correctness of fitting. It should be noted that the weak water lines not observed in our study have been neglected during the selection of transparent windows. This study might provide some references for *in situ* detection.

This work was supported by the China Postdoctoral Science Foundation (No. 2017M610771).

References

1. P. X. Neumaier, K. Schmalz, J. Borngräber, R. Wylde, and H. W. Hübers, Analyst **140**, 213 (2015).
2. Y.-D. Hsieh, S. Nakamura, D. G. Abdelsalam, T. Minamikawa, Y. Mizutani, H. Yamamoto, T. Iwata, F. Hindle, and T. Yasui, Sci. Rep. **6**, 28114 (2016).
3. A. Tekawade, T. E. Rice, M. A. Oehlschlaeger, M. W. Mansha, K. Wu, M. M. Hella, and I. Wilke, Appl. Phys. B **124**, 105 (2018).
4. Y. D. Hsieh, H. Kimura, K. Hayashi, T. Minamikawa, Y. Mizutani, H. Yamamoto, T. Iwata, H. Inaba, K. Minoshima, F. Hindle, and T. Yasui, J. Infrared Millimeter Terahertz **37**, 903 (2016).
5. A. Roggenbuck, H. Schmitz, A. Deninger, I. C. Mayorga, J. Hemberger, R. Güsten, and M. Grüninger, New J. Phys. **12**, 043017 (2010).
6. D. M. Slocum, L. H. Xu, R. H. Giles, and T. M. Goyette, J. Mol. Spectrosc. **318**, 12 (2015).
7. Y. Sun, W. Liu, S. Wang, S. Huang, and X. Yu, Chin. Opt. Lett. **9**, 060101 (2011).
8. L. H. Xu, J. Fisher, R. M. Lees, H. Y. Shi, J. T. Hougen, J. C. Pearson, B. J. Drouin, G. A. Blake, and R. Braakman, J. Mol. Spectrosc. **251**, 305 (2008).
9. H. S. Müller, F. Schlöder, J. Stutzki, and G. Winnewisser, J. Mol. Struct. **742**, 215 (2005).
10. L. S. Rothman and I. Gordon, "Steps for converting intensities from the JPL (or CDMS) catalog to HITRAN intensities," https://www.cfa.harvard.edu/HITRAN/Download/Units-JPLtoHITRAN.pdf.
11. L. S. Rothman, D. Jacquemart, A. Barbe, D. Chris Benner, M. Birk, L. R. Brown, M. R. Carleer, C. Chackerian, Jr., K. Chance, L. H. Coudert, V. Dana, V. M. Devi, J.-M. Flaudh, R. R. Gamache, A. Goldman, J.-M. Hartmann, K. W. Jucks, A. G. Maki, J.-Y. Mandin, S. T. Massie, J. Orphal, A. Perrin, C. P. Rinsland, M. A. H. Smith, J. Tennyson, R. N. Tolchenov, R. A. Toth, J. Vander Auwera, P. Varanasi, and G. Wagner, J. Quant. Spectrosc. Radiat. Transfer **96**, 139 (2005).
12. G. Herzberg, *Infrared and Raman Spectra of Polyatomic Molecules* D. Van Nostrand Company, Inc. (1945).
13. Y. Yang, A. Shutler, and D. Grischkowsky, Opt. Express **19**, 8830 (2011).